



3rd International Conference on Material and Component Performance
under Variable Amplitude Loading, VAL2015

On the use of NASGRO software to estimate fatigue crack growth under variable amplitude loading in aluminium alloy 2024-T351

B. Moreno^a, A. Martin^a, P. Lopez-Crespo^a, J. Zapatero^a, J. Dominguez^{b*}

^aUniversity of Malaga, Civil and Materials Engineering, MALAGA 29071, Spain.

^bUniversity of Seville, Department of Mechanical Engineering, Seville, Spain.

Abstract

This work uses the strip yield model implemented in NASGRO software to estimate fatigue life under random loading. Simulated results were compared with experimental data previously obtained by the authors using different random loading processes in Al2024-T351. Test data under constant amplitude loading from different authors have been considered in order to characterize the material behaviour and fit the model parameters. The two different strip yield model implemented in NASGRO software were considered. The ratio of simulated to experimental fatigue lives was between 0.71 and 1.52 considering all options and between 0.87 and 1.12 with the best option.

© 2015 The Authors. Published by Elsevier Ltd. This is an open access article under the CC BY-NC-ND license (<http://creativecommons.org/licenses/by-nc-nd/4.0/>).

Peer-review under responsibility of the Czech Society for Mechanics

Keywords: Random loading; strip yield model; NASGRO software; aluminium alloy 2024-T351

1. Introduction

In many cases of fatigue design of mechanical components, especially those whose design is based on damage tolerance, having reliable crack growth prediction tools is vital. During the past 30 years, many different models have been proposed to predict the behaviour of cracks under irregular or random loads. An important group are the models of plasticity induced crack closure or strip yield models (SYM). Several software programs, such as FASTRAN [1]

* Corresponding author. Tel.: +34 954 481 367.

E-mail address: jaime@us.es

and NASGRO [2] have been developed to implement these models. One of the most common differences between SYM is the use of the constraint factors to take into account the three-dimensional stress states. In general, SYMs determine the crack opening stress (and the opening stress intensity factor, K_{op}) evolution during the crack growth and, at the same time, use a crack growth law according to the effective stress intensity factor, $\Delta K_{eff} = K_{max} - K_{op}$. It has been found that the constraint factors in the SYM and the fitting procedure of the crack growth law to experimental data has a great influence in the predicted results [3-6]. For the same material and stress states, different values and evolution of the constraint factors, as well as, different fitting procedure and crack growth laws can be found in the literature [3-9].

The objective of the present paper is to evaluate the performance of the strip yield models implemented in NASGRO to estimate fatigue crack growth under random loading by comparing the simulated results with experimental data previously obtained by the authors. The two different SYMs available in the software and two different input crack growth data, the NASGRO equation and the discrete form in terms of da/dN vs ΔK_{eff} , have been used.

The outline of the paper is as follows. Firstly, the experimental data of fatigue crack growth under random and constant amplitude loadings are presented. Secondly, some brief comments on the strip yield models implemented in NASGRO software are included. Then, the fitting procedures for the input crack growth data are presented. Afterwards, the results and the most outstanding aspects are discussed and finally some conclusions are drawn.

2. Experimental data of fatigue crack growth under random loading

The experimental results obtained previously by the authors in crack growth tests under random loading conditions have been used [4, 10]. The tests were carried out on CT specimens of 2024-T351 aluminium alloy, with $W=50$ mm and $B=12$ mm. In all tests, cracks were allowed to grow from an initial length $a_0=15$ mm to a final length $a_f=25.3$ mm. Crack length was monitored using the ACPD method.

Tests were run by using load histories corresponding to four stationary Gaussian random processes that were characterized by different shapes of the power spectral density function [psdf, $S(\omega)$] of the loads. Table 1 shows the values of the parameters defining the four psdfs (designated A, B, C and D), as well as, the irregularity parameter, ε , which is a measure of the random process bandwidth. It represents the ratio of the mean of crossing the mean level with positive slope to the mean frequency of peaks. Figure 1a shows the shape of the spectral density functions used.

Table 1. Parameter values for the psdfs of load used.

Type	H1/H2	ω_1	ω_2	ω_3	ω_4	ε
A	6.67	5	15	80	130	0.64
B	2	5	25	30	60	0.70
C	2	10	20	25	75	0.77
D	-	7	27	-	-	0.85

Two different load levels, represented by the root mean square of the random processes (the area under $S(\omega)$ curve), were chosen. The two load levels (designated L (low) and H (high)) and the four psdfs were used to define seven stationary Gaussian random processes with zero mean. Subsequently, a constant load (4850 N) was added to prevent compression loads. Twenty different random load histories consisting of 25,000 cycles were generated for each random process. Figure 1b and c shows peaks-valleys sequence for process AH and AL.

Each load history generated was applied to a different specimen and repeated uninterruptedly until reaching the final crack length. The crack growth curves ($a-N$) were obtained throughout the process. Each load history will henceforward be designated by the code XY_Z, where X will be A, B, C or D, depending on the bandwidth of the random loading process, Y represents the load level (L low or H high) and Z represents the order number of the history within the group. Further details of tests and loading histories generation process can be found herein [10, 16].

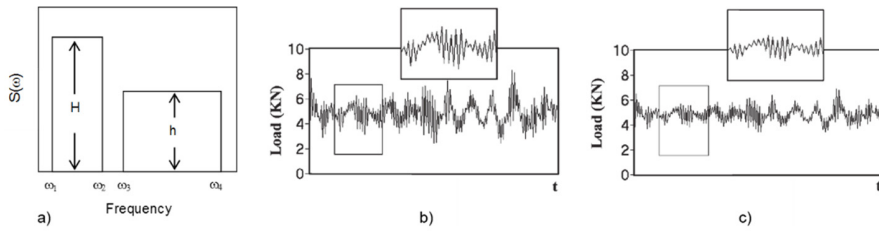


Fig. 1. (a) Shape of the spectral density functions used; (b) peaks-valleys sequence for process AH; (c) peaks-valleys sequence for process AL

Table 2 shows the statistical parameter: mean (μ) and standard deviation (σ) of the number of cycles corresponding to the growth lives obtained in each test series.

Table 2. Statistical parameter of the crack growth lives obtained in the test series considered.

Series	μ (cycles)	σ (cycles)	Series	μ (cycles)	σ (cycles)
A-H	277,151	13,377	A-L	1,163,986	35,447
B-H	197,114	7,686	-	-	-
C-H	168,287	5,124	C-L	690,667	17,715
D-H	146,981	5,363	D-L	589,569	24,525

3. Experimental data of fatigue crack growth under constant amplitude loading

Also, crack growth tests under constant amplitude loading at four different stress ratios ($R=0.1, 0.3, 0.5$ and 0.7) were carried out with the same material and specimen geometry. All specimen were precracked from an initial crack length of 10.6 mm (which is the notch length) to 12 mm. Then a constant amplitude sine load was applied from a_0 to a_f and the $a-N$ curves were recorded. All data of this test are presented in table 3. Three tests were conducted for each R value. The fatigue crack growth rates were calculated in accordance with ASTM E647. Figure 2 shows the da/dN vs ΔK results.

Table 3. Constant amplitude loading data.

R	σ_{max} (N)	σ_{min} (N)	a_0 (mm)	a_f (mm)
0.1	8.33	0.83	12	30
0.3	9.33	2.8	12	29
0.5	14.17	7.083	12	26.7
0.7	2.083	14.58	12	22.5

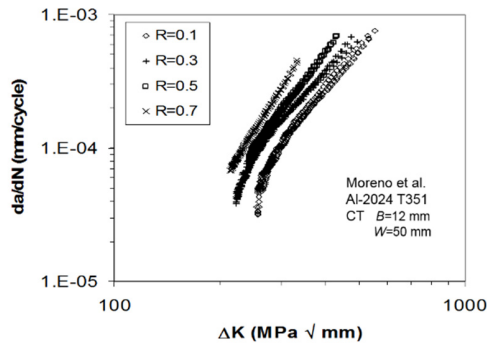


Fig. 2. Crack growth rates against stress intensity factors for constant amplitude tests

4. Strip Yield Model (SYM)

This section describes some details of the SYM implemented in the NASGRO software [2]. SYM is a mechanical model based on the assumption that a growing fatigue crack will propagate through the crack tip plastic region, and that this plastic deformation left in the wake of the crack will contribute to stress interaction effects such as stress-level dependence and crack growth rate acceleration and retardation. The concept of stress intensity factor at which the crack opens (K_{open}) and effective stress intensity factor range ($K_{eff} = K_{max} - K_{open}$) are used in the model. The SYM in NASGRO calculates a value for K_{open} by using a crack-opening model based on the Dugdale strip-yield model [11] but modified to leave plastically deformed material in the crack wake. Dugdale's original strip-yield model was defined only for thin sheets, i.e., under plane stress conditions. To accommodate a more general state of stress in strip-yield models, the local yield stress is elevated by a tensile constraint factor α .

NASGRO contains two distinct implementations of the SYM. In the first model (CCL), the tensile constraint factor α is constant along the elements of the plastic zone, but its value depends on the state of stress, ranging from plane strain to plane stress. This constraint loss is based on the observation that cracks which start initially with a flat face eventually grow in a slant face mode. Newman proposed that the transition occurs when the cyclic plastic zone size (calculated from ΔK_{eff}) reaches a percentage of the specimen thickness:

$$(\Delta K_{eff})_T = \mu \sigma_0 \sqrt{B} \quad (1)$$

where μ is the proportionality coefficient, σ_0 is the flow stress (average of yield and ultimate), B is the specimen thickness, and $(\Delta K_{eff})_T$ is the effective stress intensity factor at transition. He found that a value of 0.5 for μ was suitable for a range of materials within a $\pm 20\%$ scatter band for thin sheet. The constraint value does not change abruptly but there is a transition region which extension has been estimated conservatively at 1.0 decades of rate. Compressive constraint factors both in the plastic zone and in the crack wake are assumed to be unity for all materials.

In the second model (VCL), the tensile constraint factor α varies along the elements of the plastic zone according to a parabolic expression. The constraint decays spatially from its value at the crack tip (α_{tip}) to a plane stress value of 1.15 at the forward end of the plastic zone. Constraint loss is also built into this option, but in contrast to the model above, the plane strain or plane stress tensile value of α_{tip} is calculated from the ratio of plastic zone size to specimen thickness. This relates the constraint loss to K_{max} , whereas the CCL model relates it to ΔK_{eff} . The compressive constraint factors in the plastic zone and in the crack wake are spatially constant, and their values are given by $\alpha_{tip}/\alpha_{new}$ and $1/\alpha_{new}$, respectively, where the material parameter α_{new} characterizes the ratio of tensile tip constraint to compressive constraint.

In addition, the crack growth rate calculations in NASGRO can use different crack growth law descriptions, equations or tables. In this analysis, two different law descriptions, the NASGRO equation and a discrete form, have been used.

5. Fitting procedure of the NASGRO crack growth rate equation parameters

The crack growth rate equation used by NASGRO is:

$$\frac{da}{dN} = C \left[\left(\frac{1-f}{1-R} \Delta K \right) \right]^n \frac{\left(1 - \frac{\Delta K_{th}}{\Delta K} \right)^p}{\left(1 - \frac{K_{max}}{K_c} \right)^q} \quad (2)$$

where C , n , p and q , are the parameters of the material to be adjusted, R is the load ratio, $\Delta K_{eff} = K_{max} - K_{op}$ and ΔK_{th} are the effective and threshold stress intensity factor ranges, respectively, and K_{max} , K_{op} and K_c are the maximum, crack opening and critical stress intensity factors, in that order. The function f is $f = K_{op}/K_{max}$.

NASGRO includes the software module NASMAT to store and curve-fit the crack growth rate data. This module allows to fit the $da/dN-\Delta K$ equation to a group of constant amplitude test data. To assess the function f in this fitting module, the crack opening function defined by Newman [12] was used. This function depends on the constraint factor, α , which has been treated here as a constant for the purpose of fitting the crack growth data.

The present authors [6] made different adjustments with NASMAT by changing the p and q exponents, the R of CA test used to fit, and the constraint factor α in order to study the influence of those parameters in the crack growth rate law obtained. The main conclusions of that analysis were the following:

- The adjustment of the growth rate equation to the diverse stress ratio test groups (R) results in marked variations in the fitted parameters and therefore in the growth prediction.
- The constraint factor used in the adjustment has the largest influence on the fitted parameters obtained and therefore in the growth prediction.
- The module NASMAT does not provide any tool to define the best fit.
- It is possible to obtain different sets of parameters (c , n , p and q) which produce similar crack growth rates.

The fitting efficiency was determined by comparing the estimates with experimental data of crack growth with CH process and VCL option. The set of parameters for the NASGRO equation which provided the best fit to random loading test was selected (table 4). It was obtained by using a constraint factor $\alpha=2$. This α value is in concordance with the plane strain state that can be assumed for the material and specimen geometry herein. From the total of twenty loading histories, the ones with the longest and shortest lives have been chosen for the comparison. These loading histories are those that present the highest and lowest retardation effects. In this paper the simulated results with these parameters for the seven considered processes and both SYM options in NASGRO (CCL and VCL) are presented in the results section.

Table 4. Crack Growth Eqn Constants (S.I. Units: mm, MPa, MPa mm^{1/2}).

C	n	p	q	DK ₀	Cth+	Cth-	Rcl	Alpha	Smax/SIG ₀
0.174D-10	2.824	0.5	0.5	124.86	2.5	0.10	0.70	2.00	0.30

6. Crack growth rate law discrete form

One of the most problematic or questionable aspects of the previous section is that the available data of constant amplitude correspond to a narrow range of crack growth rates or ΔK values. In order to improve this and therefore the characterization of the material behavior, other author's data as well as NASGRO material database has been used to generate a da/dn vs ΔK_{eff} curve.

Figure 3a shows the rate data vs ΔK on the 2024-T351 tests conducted by Donald and James [13] as well as previous data obtained by authors, which agree very well with Donald's data. The shape of these curves also show a nonlinear ΔK -rate relationship, this implies that the NASGRO equation can not reproduce this trend. Figure 3a data can be converted into da/dn vs ΔK_{eff} curves using Newman's crack-opening stress equation [12]. Figure 3b shows these data obtained by assuming a constraint factor $\alpha=2$ and $S_{max}/\sigma_0=0.1$. The NASA ΔK_{eff} -rate curve [14] and the NASGRO material database curve for Al-2024-T351 are also shown in figure 3b. It is seen a good correlation for fatigue crack growth rate data over a wide range of rates except near the threshold regime. In that regime, the results on the compact specimens were determined by using a load-reduction procedure, it has been shown that the load-reduction procedure may induce higher thresholds due to higher crack-closure behavior [15]. The NASA curve is drawn to highlight the differences found in the literature and it has been used to analyze the influence of the threshold in the results.

A da/dn vs ΔK_{eff} curve baseline relation (table 5) was chosen to fit these data and used as a table-lookup input. This baseline curve is over the band of data between 1E-6 mm/cycle and 1E-3 mm/cycle and has the same values as the NASGRO database line below 1E-6 mm/cycle (in the threshold regime) and above 1E-3 mm/cycle. A detail of this curve together NASGRO database line is showed in the results section.

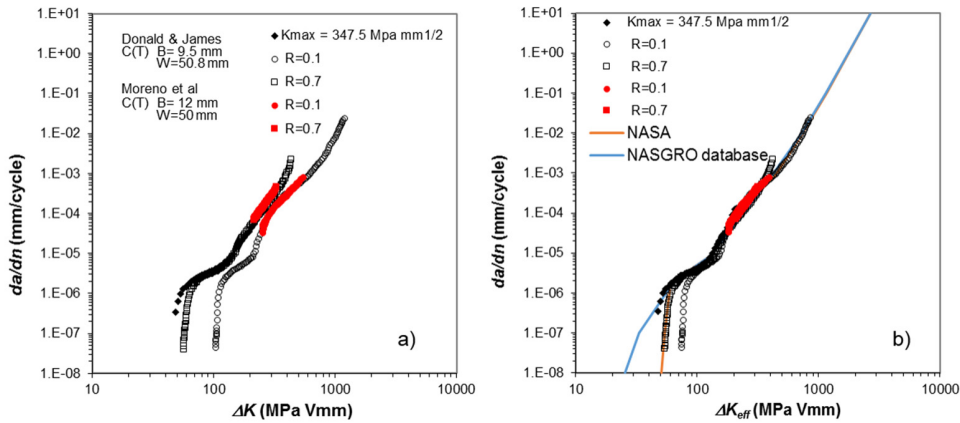


Fig. 3. (a) Crack growth rates against stress intensity factors, (b) crack growth rates against effective stress intensity factors.

Table 5. da/dn vs ΔK_{eff} curve baseline relation

ΔK_{eff} (MPa m ^{1/2})	da/dN (mm/cycle)	ΔK_{eff} (MPa m ^{1/2})	da/dN (mm/cycle)
25.30	1.00E-08	215.00	6.00E-05
33.20	1.00E-07	557.00	2.10E-03
64.83	2.00E-06	764.00	1.10E-02
110.00	8.00E-06	1170.00	1.00E-01
140.00	1.70E-05	2687.00	1.00E+01

7. Results and discussion

The SYMs from NASGRO have been applied to predict fatigue crack growth under constant amplitude and random loading. The computation carried out includes both SYM options, CCL and VCL, as well as the two descriptions of the crack growth law, the NASGRO equation parameters and the discrete form in terms of da/dN vs ΔK_{eff} . For the discrete form two different curves have been used, the NASGRO database table for Al-2024-T351 and the baseline previously listed (table 5).

For the CCL option, a tensile constraint factor $\alpha = 2$ was chosen, since the material is aluminum and the specimen is 12 mm thick, corresponding to plane strain state. This α value is consistent with the corresponding value used in the fitting procedure of the NASGRO equation parameters and the procedure used to generate the da/dN vs ΔK_{eff} curve. The effective stress intensity factor at transition is $(\Delta K_{eff})_T = 710 \text{ MPa mm}^{1/2}$ from equation (1). The extent of the transition region has been estimated at one decade of rate, from an initial rate $da/dN = 0.9E-2 \text{ mm/cycle}$. However, the analysis performed showed that the upper $(\Delta K_{eff})_T$ regime is not reached (except in some very high peak of high load processes and long cracks) and therefore the model essentially uses a constant constraint factor.

For the VCL option, NASGRO manual recommend to fit α_{new} from comparisons of predictions with selected constant-amplitude and spike load sequences. As these test data are not available, comparisons with the loading histories that present the highest and lowest retardation effects have been used to fit the α_{new} parameter. Different values of α_{new} varying from 1 to 3 have been considered herein and insignificant differences have been found. All results in this section have been obtained with $\alpha_{new} = 2$.

To analyze the influence of near threshold regime data on the simulation results, two different comparisons have been made. A comparison of the results obtained using the NASGRO equation parameters for different ΔK_{th} values and a comparison of the results obtained using the NASA and NASGRO database curves, which differ mainly in the threshold. This analysis has shown that higher threshold values produce longer lives but maximum differences are below 10%.

According to commonly applied criteria for the evaluation of predicted results, the ratio of the estimated life (N_{NASGRO}) to the experimental fatigue life (N_{EXP}) have been obtained. The results for constant amplitude and random loading are summarized in figure 4, for random loading the value corresponds to the average results of the twenty loading histories of each process (840 simulations).

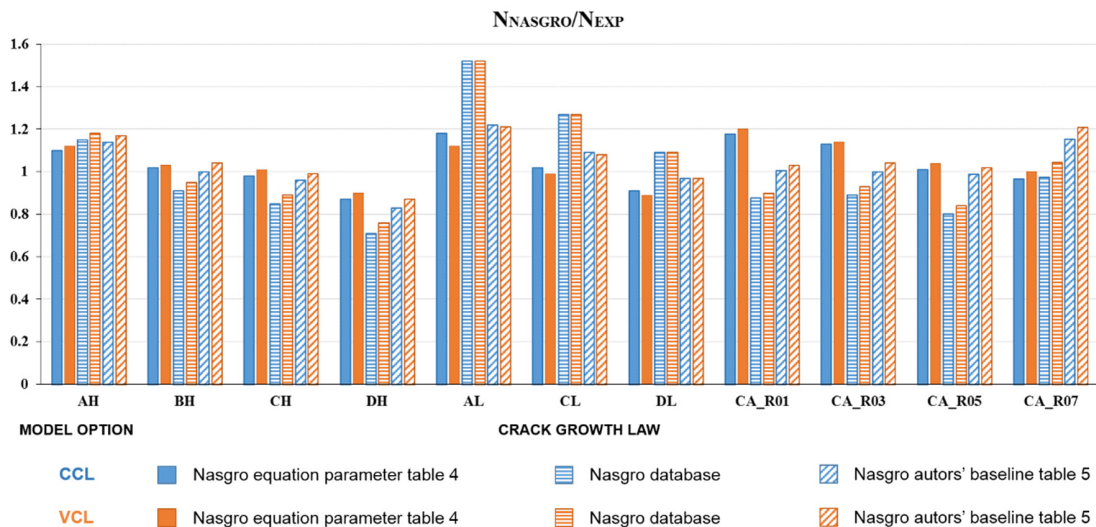


Fig. 4. Ratio of the estimated number of cycles until final crack length to the experimental fatigue life, N_{NASGRO}/N_{EXP} .

Previous results show that for constant amplitude loading the best results correspond to the ones obtained by using the crack growth law proposed by the authors in table 5, which improve the results corresponding to the ones obtained by using the nasgro database law. The results obtained by using the nasgro equation, with the parameters listed in table 4, are not so good for low stress ratio because of the curved shape of the relationship da/dN vs ΔK (see fig. 2). Figure 6a show the experimental and simulated a-N curves for two stress ratios.

Figure 4 shows that both models predict very similar growth lives. For the processes herein, the CCL model uses a constant constraint factor α because the constraint-loss regime is never achieved. On the other hand, the calculated value of the tensile constraint factor in the VCL model is constant too because the specimen thickness is quite bigger than the plastic zone. These results could be substantially different for a smaller thickness specimen

For random loading, the previous results show good predictions for all processes and options, the ratio N_{NASGRO}/N_{EXP} is between 0.71 and 1.52; ratios are higher for low load level processes (L) than for high ones (H). The predictions tend to be conservative for high load level processes (except AH) and non-conservative for low load level processes. In general, the ratios closest to unity correspond with those obtained by using the nasgro equation with the parameters of table 4, this is a consequence of the fitting procedure used, described in section 5. It should be considered that the fitting of this law was obtained by a trial-error iterative procedure whose efficiency was determined by comparing simulated and test results under random processes.

For the description of the crack growth law in the discrete form, the authors' baseline (relationship da/dN vs ΔK_{eff}) proposed in table 5 improves the results obtained by using the NASGRO database table, except for process AH. The best results were obtained for the high load level processes BH, CH and DH. In these processes, more than 90% of the load ranges produce stress intensity factor ranges from $\Delta K=70$ MPa $\sqrt{\text{mm}}$ for the initial crack length to $\Delta K=420$ MPa $\sqrt{\text{mm}}$ for the final crack length. Considering this range of ΔK values and transforming them to ΔK_{eff} , from figure 3b, a range of crack growth rates from $3.0E-5$ to $2.0E-4$ mm/cycle can be estimated. This may indicate that the crack growth rates in that range are well characterized by the da/dn vs ΔK_{eff} relations used. Figure 5a represents the evolution of the calculated crack growth rate from test data for the load histories of series CH with the shortest and longest lives, CH-09 and CH-11 respectively. These loading histories are those that present the highest and lowest retardation effects. Figure 5b compares the evolution of the calculated crack growth rate from the a-N curves obtained

experimentally and with nasgro (model option VCL and the crack growth law listed in table 5), it shows that the model follows very well the evolution of the growth rates, and detects the retardation effect of the overloads, although this effect is underestimated as the crack grows. Figures 6b and 6c show the a-N curves obtained by test and nasgro (VCL and CCL options). The not so good results for low load level processes AL, CL and DL could be because crack growth rates are in a lower range. For these processes the 90% of the load ranges produce stress intensity factor range from $\Delta K=30 \text{ MPa } \sqrt{\text{mm}}$ for the initial crack length to $\Delta K=250 \text{ MPa } \sqrt{\text{mm}}$ for the final crack length. Figure 3a shows that this range of ΔK values is well in the zone of ΔK_{th} , where the uncertainty of the crack growth rate is high. This indicates that the crack growth rates in this range are not so well characterized.

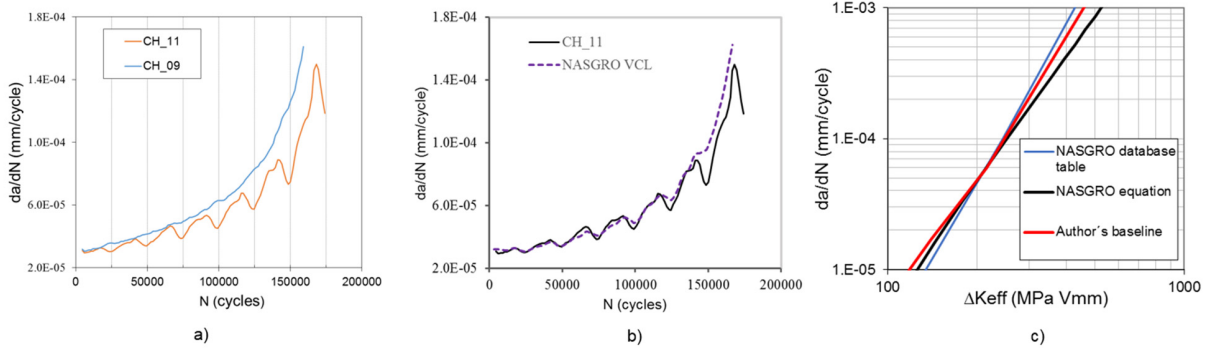


Fig. 5. (a) Evolution of the crack growth rate in test for two different load histories of CH process; (b) Evolution of the crack growth rate in test and nasgro for load history CH-11; (c) Detail of da/dN vs ΔK_{eff} curves.

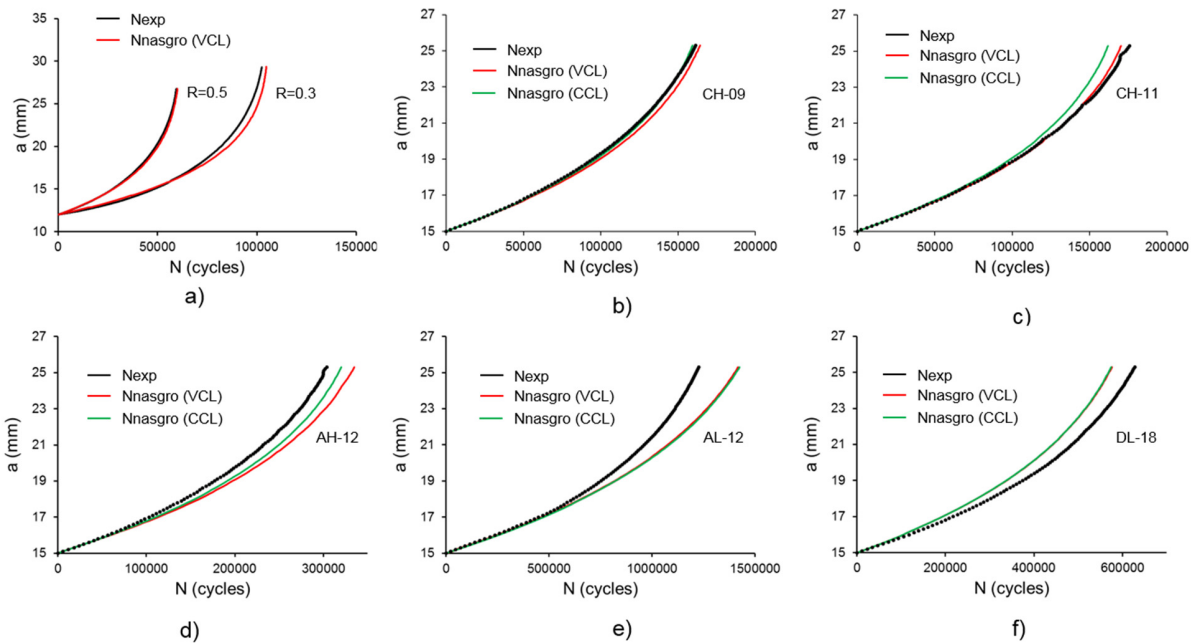


Fig. 6. Experimental and simulated a-N curves for different process. All curves were obtained by using the crack growth rate law listed in table 5.

If the NASGRO equation with parameters of table 4 is converted into a da/dN vs ΔK_{eff} curve, it can be drawn on the same graph together to the NASGRO database table for AI-2024-T351 and the authors' baseline (table 5). A detail of these curves in the region of interest is showed in Figure 5c, which shows that all curves are very similar in this region. This fact justifies the acceptable results obtained using any one of them.

Figure 6 shows the experimental and simulated a - N curves for some of the load histories applied. All simulated curves there shown have been obtained by using the crack growth rate law listed in table 5. Figures 6a show the comparison between the experimental and simulated a - N curves for constant amplitude loadings. Figures 6d to 6f show the comparison between the experimental and simulated a - N curves for other three cases here analyzed. A good agreement between the computed and measured crack growth rates can be observed.

8. Conclusions

The main conclusions of the study to stand out are:

- All models and crack growth rate laws here considered allow to obtain a reasonable agreement ($N_{\text{NASGRO}}/N_{\text{EXP}}$ is between 0.71 and 1.52). The results herein obtained for both model options, CCL and VCL, are very similar.
- The best results (with $N_{\text{NASGRO}}/N_{\text{EXP}}$ between 0.87 and 1.12) correspond with the NASGRO equation option, but this is a consequence of the fitting procedure used.
- The law proposed by the authors (table 5) improves the results obtained by using the NASGRO database table. The ratio $N_{\text{NASGRO}}/N_{\text{EXP}}$ is between 0.82 and 1.42 for the proposed law while $N_{\text{NASGRO}}/N_{\text{EXP}}$ is between 0.71 and 1.52 for the NASGRO database table. The best predictions were obtained for processes BH, CH and DH with a ratio $N_{\text{NASGRO}}/N_{\text{EXP}}$ between 0.82 and 1.03 by using the data of table 5, while, $N_{\text{NASGRO}}/N_{\text{EXP}}$ is between 1.02 and 1.42 for AH, AI, BL and CL processes.

Acknowledgements

Financial support of Spanish Ministerio de Economía y Competitividad through grant reference DPI2012-33382 and of Junta de Andalucía through Proyectos de Excelencia grant reference TEP-3244 is greatly acknowledged.

References

- [1] Newman Jr JC. FASTRAN II—a fatigue crack growth structural analysis program. NASA TM 104159, 1992.
- [2] NASGRO, Fracture mechanics and fatigue crack growth analysis software (version 6.0), reference manual, NASA Johnson Space Center and Southwest Research Institute; 2010.
- [3] Zapatero J, Moreno B, Domínguez J. On the use of the strip-yield model to predict fatigue crack growth under irregular loading. *Fatigue Fract Engng Mater Struct*, 1997, 20:759-770.
- [4] Zapatero J, Moreno B, Gonzalez-Herrera A, Domínguez J. Numerical and experimental analysis of the fatigue crack growth under random loading. *International Journal of Fatigue*. 2005;27:878-890.
- [5] Skorupa M, Machniewicz T, Schijve J, Skorupa A. Application of the strip-yield model from the NASGRO software to predict fatigue crack growth in aluminium alloys under constant and variable amplitude loading. *Engineering Fracture Mechanics*. 2007;74:291-313.
- [6] Moreno B, Zapatero J, Lopez-Crespo P, Domínguez J. On the application of the strip-yield model from NASGRO and FASTRAN software for fatigue crack growth under variable amplitude loading. *Proceedings of 2nd International Conference on Material and Component Performance under Variable Amplitude Loading*. Darmstadt, Germany; 2009.
- [7] Yamada Y, Lacy T, Newman JC, Smith BL, Kumar B. Effects of crack closure on fatigue crack-growth predictions for 2024-T351 aluminum alloy panels under spectrum loading. *International Journal of Fatigue*. 2007;29:1503–1509.
- [8] Christopher D. Glancey, Robert R. Stephens, Fatigue crack growth and life predictions under variable amplitude loading for a cast and wrought aluminum alloy, *International Journal of Fatigue*, 2006, 28:53–60.
- [9] F.J. McMaster, D.J. Smith, Predictions of fatigue crack growth in aluminium alloy 2024–T351 using constraint factors, *International Journal of Fatigue*, 2001, Pages 23–93–101
- [10] Moreno B, Zapatero J, Domínguez J. An experimental analysis of fatigue crack growth under random loading. *International Journal of Fatigue*. 2003;25:597-608.
- [11] Dugdale DS. Yielding of steel sheets containing clits. *J Mech Phys Solids* 1960;8:100–4.
- [12] Newman JC. A crack opening stress equation for fatigue crack growth. *International Journal of Fracture*. 1984;24(3):R131-R135.
- [13] Donald K, James M. Private communication. Alcoa; 2009.
- [14] Newman JC, Phillips EP, Swain MH. Fatigue-life prediction methodology using dsmall-vrack theory and a crack-closure model. *Proceedings of FAA-NASA Symposium on the Continued Airworthiness of Aircraft Structures*, DOT/FAA/AR-97/2, p 331-356; July 1997.
- [15] Newman JC, Brot A, Matias C. Crack-growth calculations in 7075-T7351 aluminum alloy under various load spectra using an improved crack-closure model. *Engineering Fracture Mechanics*. 2004; 71:2347–2363.

- [16] Zapatero J, Jose Pascual J, Dominguez J, Effect of load histories on scatter of fatigue crack growth in aluminum alloy 2024-T351. *Engineering Fracture Mechanics*, 1997, 56:67-76.